Holographic Superfluids and the Dynamics of Symmetry Breaking

M. J. Bhaseen, J. P. Gauntlett, B. D. Simons, J. Sonner, and T. Wiseman

Holographic Superfluids and the Dynamics of Symmetry Breaking

M. J. Bhaseen,[1] J. P. Gauntlett,[2] B. D. Simons,[1] J. Sonner,[3] and T. Wiseman[2]

[1]*Cavendish Laboratory, University of Cambridge, Cambridge, CB3 OHE, U.K.*
[2]*Blackett Laboratory, Imperial College, London SW7 2AZ, U.K.*
[3]*DAMTP, University of Cambridge, CB3 OWA, U.K.*

We explore the far from equilibrium response of a holographic superfluid using the AdS/CFT correspondence. We establish the dynamical phase diagram corresponding to quantum quenches of the order parameter source field. We find three distinct regimes of behaviour that are related to the spectrum of black hole quasi-normal modes. These correspond to damped oscillations of the order parameter, and over-damped approaches to the superfluid and normal states. The presence of three regimes, which includes an emergent dynamical temperature scale, is argued to occur more generally in time-reversal invariant systems that display continuous symmetry breaking.

In the last few years there has been a wealth of experimental activity exploring the non-equilibrium properties of quantum many body systems. Recent advances include observations of long-lived oscillations in colliding Bose gases [1], and the dynamics of cold atoms following a quantum quench [2, 3]. Non-equilibrium measurements have also been exploited to reveal the superfluid amplitude mode [4], and to explore pairing in high temperature superconductors [5]. In parallel there has also been significant theoretical work on low-dimensional strongly correlated systems, where analytical [6] and numerical [7–9] progress is possible; for a review see Ref. [10].

A notable feature to emerge from the dynamics of the integrable BCS (Bardeen–Cooper–Schrieffer) Hamiltonian, following an abrupt quench of the pairing interactions, is a regime of persistent oscillations of the order parameter [11–15]. This is accompanied by a transition to a regime of damped oscillations as the quench strength is increased [16]. These integrable results apply in the collisionless regime, for timescales shorter than the energy relaxation time [17, 18]. In spite of these achievements, it is challenging to see how such results are modified at late times in the collision dominated regime. In particular, do the oscillations and the transition withstand quantum and thermal fluctuations and departures from integrability? Related considerations apply to other integrable systems, and generalizing non-equilibrium results to more generic situations, including higher dimensions, is a major open challenge.

In this respect, the AdS/CFT (anti-de Sitter/conformal field theory) correspondence [19–21] can offer valuable insights. It recasts certain strongly interacting quantum systems, which are large N field theories, in terms of weakly coupled gravitational models in at least one dimension higher. This provides access to the quantum dynamics from the classical gravitational equations, where finite temperatures correspond to black hole solutions [22–27]. The methods are very powerful when combined with numerical solution of the equations of motion, as they allow access to the far

from equilibrium response over the entire time evolution [28–33].

In this manuscript we will focus on the dynamics of a holographic superfluid [29, 34, 35] under a spatially homogeneous and isotropic quench. Our primary aim is to reveal three regimes of non-equilibrium response, including a dynamical transition from under-damped to over-damped collective oscillations. We argue that this transition will feature in other (holographic and non-holographic) time-reversal invariant systems that display continuous symmetry breaking.

Model.— We consider the simplest representative action for a holographic superfluid, originally introduced in Refs. [34, 35]. The model is defined in the so-called "bottom-up" approach which specifies the action directly on the gravitational side, without recourse to microscopic string theory calculations. It describes a complex scalar field ψ, with charge q and mass m, minimally coupled to electromagnetism and gravity in 3+1 dimensions:

$$ S = \frac{1}{2\kappa^2} \int d^4x \sqrt{-g} \Big[R + \frac{6}{\ell^2} - \frac{F^2}{4} - |D\psi|^2 - m^2 |\psi|^2 \Big], \quad (1) $$

where $F_{ab} = \partial_a A_b - \partial_b A_a$, $D_a = \partial_a - iqA_a$, and the radius ℓ parameterizes the inverse curvature of AdS space-time.

Exploiting the AdS/CFT correspondence, the model is dual to a strongly coupled large N CFT in 2+1 D flat Minkowski space-time, residing on the AdS boundary, as shown in Fig. 1; for reviews see Refs. [36, 37]. The CFT is time-reversal invariant and has a global U(1) symmetry whose conserved current, J_μ, is dual to A_a. The U(1) symmetry is spontaneously broken below a critical temperature, T_c, corresponding to the onset of superfluidity. This is possible in the 2+1 D CFT due to large N [35]. Other holographic superfluid models, including 3+1 D CFTs, will exhibit analogous phenomena. In this manuscript we set $1/(2\kappa^2) \equiv \mathcal{C}/\ell^2$ and choose units with $\ell = 1$. Here, $\mathcal{C}$ is a measure of the number of local degrees of freedom in the CFT, with $\mathcal{C} \sim N^{3/2}$ at large N.

In general, it is very difficult to analyse such strongly interacting high dimensional CFTs, but the AdS/CFT

corrrespondence allows key insights. In particular, fields in AdS space-time may be related to physical obervables in the CFT via their coordinate expansion close to the AdS boundary. Assuming spatial homogeneity and isotropy of the boundary theory, the holographic description requires two coordinates, z and t; here z parameterizes the distance from the AdS boundary and t is the boundary time, as shown in Fig. 1. For example, in equilibrium the time-component of the gauge field, A_t, is dual to the charge density ρ of the CFT, via the expansion $A_t = \mu - z\rho + \dots$, where μ is the chemical potential of the CFT with $\langle J_t \rangle = \rho/2\kappa^2$. Likewise, the field ψ is dual to an operator $\mathcal{O}$ in the CFT. Using the standard holographic dictionary, this has a scaling dimension Δ fixed by m [34, 35]; for simplicity, we choose $q = 2$ and $m^2 = -2/\ell^2$ with $\Delta = 2$ [38]. This corresponds to the expansion $\psi = z\psi_1 + z^2\psi_2 + \dots$, with $\psi_1 = 0$. Analogous to the previous identifications, the AdS/CFT correspondence allows one to identify ψ_1 as a source for the operator $\mathcal{O}$, and ψ_2 as the expectation value, $\langle \mathcal{O} \rangle \equiv \psi_2/2\kappa^2$.

As highlighted in Refs. [34, 35], the operator $\mathcal{O}$ corresponds to the superfluid order parameter of the CFT, and is non-vanishing below T_c. In the gravitational framework, this reflects a change in the classical black hole solutions of the model (1); in the normal state the black holes have $\psi = 0$, whilst in the superfluid state they have "scalar hair" with $\psi \neq 0$. The bosonic order parameter $\mathcal{O}$ is argued to be composed of fermionic bilinears and scalar fields residing in the 2+1 D CFT [39]. Although more complicated than in BCS theory, it is highly reminiscent of a pairing field. Whilst a detailed microscopic description of the CFT and its operator content requires a "top-down" approach based on string theory, we can nonetheless make a great deal of progress without such considerations owing to universality. We will return to string theory descriptions in future work.

Gaussian Quantum Quench.— We now analyse the far from equilibrium dynamics of the dual CFT, at finite temperature and charge density, by numerically constructing time-dependent black hole solutions for the holographic model (1). Details of our coordinate system and metric are provided in the Supplementary Material; see also Fig. 1. Near the AdS boundary at $z = 0$ the latter have the time-dependent asymptotic expansion

$$\psi = z\psi_1(t) + z^2\psi_2(t) + \dots, \quad A_t = \mu(t) - z\rho(t) + \dots \quad (2)$$

The holographic renormalization group allows one to establish the time-dependent correspondence

$$\langle J_t(t) \rangle = \frac{\rho(t) - \dot{\mu}(t)}{2\kappa^2}, \quad \langle \mathcal{O}(t) \rangle = \frac{[\psi_2(t) + 2i\mu(t)\psi_1(t)]}{2\kappa^2}, \quad (3)$$

in our space-time coordinates and gauge; in the case where $\mu = \dot{\mu} = 0$ we recover the previous correspondence. We take as our initial state a superfluid corresponding to a black hole with $\psi \neq 0$ [35], and set the initial temperature to $T_i = 0.5T_c$ for numerical convenience; as we will
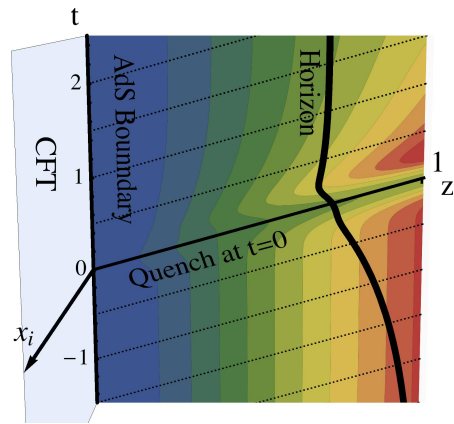

FIG. 1. Schematic representation of the coordinate system; for details see the Supplementary Material. We show data for the time evolution of $\mathrm{Re}\psi(t, z)$ following a Gaussian quench at $t = 0$ with $\delta = 0.15$, from a superfluid black hole initial state as $t \to -\infty$ with $T_i/T_c = 0.5$. The behaviour near the AdS boundary at $z = 0$ is used to extract the dynamics of the superfluid order parameter $\langle \mathcal{O}(t) \rangle$ in Figs 2,3.

see, similar results are also expected for other values of T_i. We then apply a quench of the source field $\psi_1(t)$, conjugate to $\langle \mathcal{O}(t) \rangle$. Specifically, we apply a Gaussian-type quench, centred on $t = 0$, by imposing

$$\psi_1(t) = \bar{\delta}\, e^{-(t/\bar{\tau})^2}, \quad (4)$$

where $\bar{\delta}$ and $\bar{\tau}$ characterise the quench strength and timescale respectively. The chemical potential of the initial state, μ_i, sets the scale for the resulting dynamics and explicitly breaks conformal invariance. This is nonetheless amenable to a holographic treatment and we use μ_i to define dimensionless $\delta \equiv \bar{\delta}/\mu_i$ and $\tau \equiv \mu_i\bar{\tau}$. For definiteness, we set $\tau = 0.5$ and will vary δ. We track the dynamics by solving the equations of motion of (1) numerically. As discussed in the Supplementary Material we choose a gauge for $\mu(t)$ which keeps the initial and final charge densities the same while the quench injects energy into the system. Then $\mu(t)$ interpolates from the initial value, μ_i, to a final chemical potential, μ_f. We find similar results for other values of τ, and also for quenches which do not preserve the equality of initial and final charge density. As we shall see, our quench is abrupt compared with the emergent relaxation time-scale.

Dynamical Phase Diagram.— In Fig. 2 we show the dynamical phase diagram as a function of δ. It displays three regimes of late-time behaviour whose asymptotics are governed by the gauge-invariant equation

$$|\langle \mathcal{O}(t) \rangle| \simeq |\langle \mathcal{O} \rangle_f + \mathcal{A}e^{-i\omega t}|, \quad (5)$$

where $\langle \mathcal{O} \rangle_f$ is the final order parameter, $\mathcal{A}$ is an amplitude pre-factor, and ω is a complex frequency in the lower half-plane. In region III it displays exponential decay towards a vanishing final order parameter $|\langle \mathcal{O} \rangle_f| = 0$, so

FIG. 3. Quench strength δ versus final state temperature T_f using the same initial parameters as in Fig. 2. The dynamical transition at $\delta_* \approx 0.14$ occurs within the superfluid at a temperature $T_* \approx 0.81 T_c$.
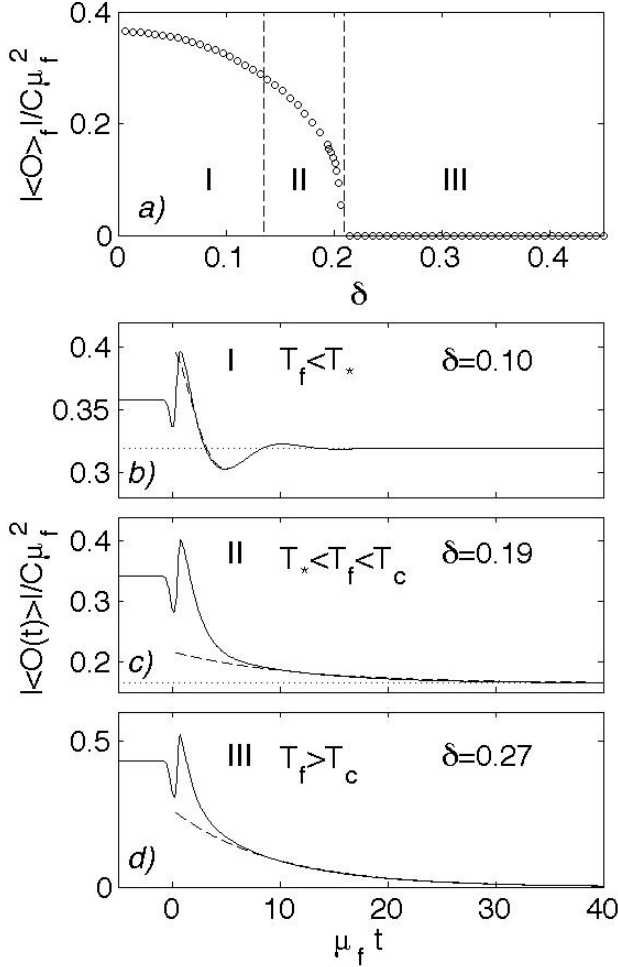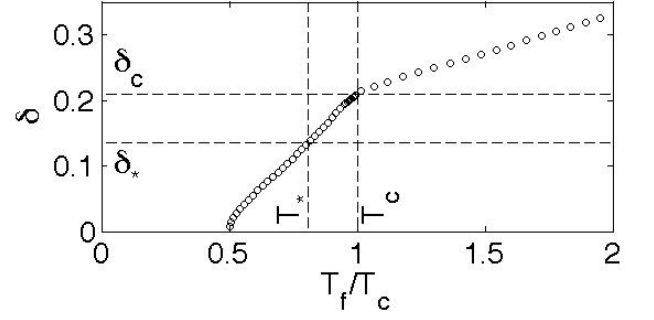
FIG. 2. (a) Dynamical phase diagram of the holographic superfluid showing the final order parameter, $|\langle \mathcal{O} \rangle_f|$, at late times. We start in the superfluid with $T_i = 0.5 T_c$, and monitor the time evolution with increasing quench strength δ. The dynamics exhibits three regimes. For the chosen parameters the transitions occur at $\delta_* \approx 0.14$ and $\delta_c \approx 0.21$. (b) In region I we observe damped oscillations towards $|\langle \mathcal{O} \rangle_f| \neq 0$. (c) In II we find a non-oscillatory approach towards $|\langle \mathcal{O} \rangle_f| \neq 0$. (d) In III we find a non-oscillatory decay towards $|\langle \mathcal{O} \rangle_f| = 0$. The dashed lines in (b), (c), and (d) correspond to the dominant quasi-normal modes of the final state black holes for temperatures $T_f/T_c = 0.73, 0.95, 1.48$ respectively.

that for large δ we exit the initial superfluid phase completely. In contrast, in region II it exhibits non-oscillatory exponential decay with $\mathrm{Re}(\omega) = 0$ towards $|\langle \mathcal{O} \rangle_f| \neq 0$. As we shall see later, this corresponds to the presence of a gapped "amplitude" mode and a gapless "phase" mode in the superfluid phase. However, in region I it exhibits exponentially damped oscillations with $\mathrm{Re}(\omega) \neq 0$ towards $|\langle \mathcal{O} \rangle_f| \neq 0$, so that for smaller δ there is another regime of dynamics. For the parameters used in Fig. 2, the transition from I to II occurs at a critical value $\delta_* \approx 0.14$, whilst the transition from II to III occurs at $\delta_c \approx 0.21$.

The behaviour shown in Fig. 2 is reminiscent of the dynamics of a BCS superconductor [16], despite the

fact that the holographic superfluid is strongly coupled, and that the effects of thermal damping are incorporated. Indeed, the persistent oscillations of the integrable BCS Hamiltonian are replaced here by an underdamped approach towards $|\langle \mathcal{O} \rangle_f| \neq 0$, whilst the power-law damped BCS oscillations are replaced by an exponentially damped approach. The transition at δ_* provides a finite temperature and collision dominated analogue of the collisionless Landau damping transition [16].

It is illuminating to consider the phase diagram as a function of the equilibrium temperature of the final state black hole, T_f. Fig. 3 shows that T_f increases monotonically with δ, as expected. Replotting the data in Fig. 2 against T_f we obtain the equilibrium phase diagram of the holographic superfluid [35], with the transition from II to III being associated with T_c, and the transition from I to II associated with an emergent temperature scale $T_* \approx 0.81 T_c$, determined by δ_*.

Quasi-Normal Modes.— To gain insight into the three regimes of collective dynamics and the temperature T_*, we examine the late time asymptotics in more detail. As $t \to \infty$, the dynamics is described by the quasi-normal modes (QNMs) of the late time black holes. Each QNM describes an approach to equilibrium in linear perturbation theory with time dependence $e^{-i\omega t}$. Those that dominate the late time dynamics have complex frequency ω closest to the real axis and give rise to the behaviour in Eq. (5). As outlined in the Supplementary Material, we have calculated the homogeneous isotropic QNMs both for the normal state black holes (see Eq. (2) of the Supplementary Material), and for the superfluid black holes of Ref. [35]. This generalises the analysis of [40] who calculated the QNMs (also for non-zero momentum) in a probe approximation. For our purposes, we need to go beyond the probe approximation and include back-reaction and the trajectories of the dominant QNMs in the complex ω plane are depicted in Fig. 4.

Typically, the real parts of the dominant QNM frequencies correspond to oscillations, and the imaginary parts to damping. However, as shown in Fig. 4(c), for
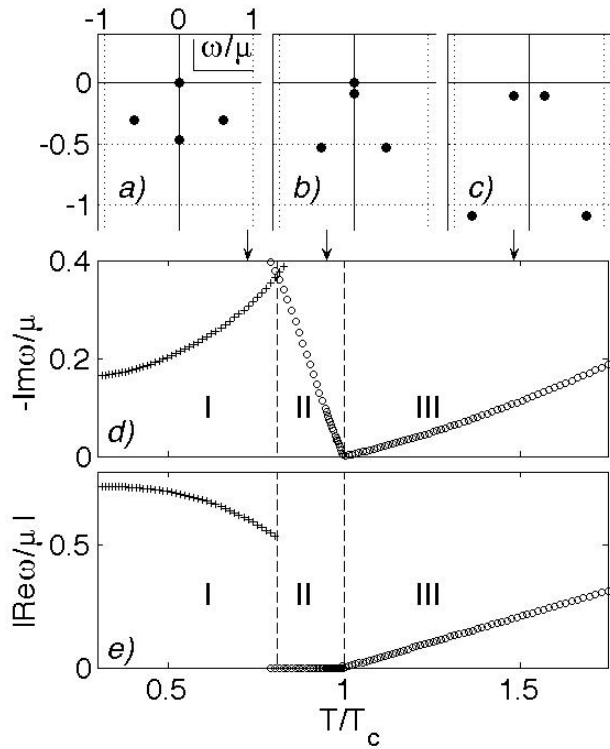
FIG. 4. Evolution of the QNM frequencies with temperature. (a) $T = 0.73T_c$. (b) $T = 0.95T_c$. (c) $T = 1.48T_c$. Time reversal invariance corresponds to $\omega \rightarrow -\omega^*$. (d) and (e) show the imaginary and real parts of the dominant QNMs. i.e. the QNMs closest to the real axis. The results show three regimes of dynamics, in quantitative agreement with Fig. 2.

$T > T_c$, the QNMs for the normal state black hole have two complex frequencies that are closest to the real axis. Nonetheless, substitution into Eq. (5) with $\langle \mathcal{O}_f \rangle = 0$ yields the damped non-oscillatory behaviour found in region III of Fig. 2. As the temperature is lowered, these dominant poles migrate upwards in the complex ω plane and at the superfluid transition temperature, T_c, they coincide at $\omega = 0$. This corresponds to spontaneous U(1) symmetry breaking with the appearance of a Goldstone mode. Below T_c, one of these modes, the "amplitude" mode, travels down the imaginary axis, consistent with time-reversal invariance under $\omega \rightarrow -\omega^*$, whilst the Goldstone "phase" mode remains pinned at $\omega = 0$; see Fig. 4(b). The amplitude mode describes the damped approach to a finite order parameter in region II of Fig. 2; the Goldstone mode does not affect the dynamics in the homogeneous and isotropic context, although it does lead to a hydrodynamic mode at non-zero spatial momentum. As the temperature is lowered, the subdominant poles also ascend in the complex plane. At the dynamical transition temperature T_*, the damping rate of the descending amplitude mode coincides with that of the ascending subdominant complex poles. For the chosen parameters this occurs at $T_* \approx 0.81T_c$, in agreement with the nonlinear analysis. Below T_*, the previously subdominant poles

now become dominant, as shown in Fig. 4(a). The dynamics corresponds to a damped oscillatory approach to a finite order parameter as found in region I. In addition to this change in dynamics at T_*, one may also extract the variation of the emergent timescales as a function of temperature. As shown in Figs. 4(d) and (e), there are three regimes. Moreover, the extracted timescales are in quantitative agreement with the late time behaviour of the nonlinear analysis, as indicated by the dashed lines in Figs. 2(b)-(d). The linear response analysis provides an excellent description over a broad time interval.

Dynamics of Symmetry Breaking.— The main results on the late time behaviour of the quenched holographic superfluids, captured in Figs. 2-4, have a more universal applicability. Recall that the location of the QNMs of the black holes presented in Fig. 4, correspond to the location of poles of the retarded Green's function for the operator $\mathcal{O}$ in the dual theory [41]. Thus, the late time behaviour is equivalently described by the poles of the retarded Green's function that are closest to the real axis. A key point is that the pole structure in Fig. 4 is the *generic* behaviour for an isotropic and homogeneous system with time-reversal invariance under $\omega \rightarrow -\omega^*$, which can spontaneously break a continuous global symmetry including the presence of the Goldstone mode at the origin and secondary quasiparticle excitations. The value of T_*, if it exists, will be given by the temperature at which the value of $\text{Im}(\omega)$ for the pole on the imaginary axis, and those poles off the imaginary axis and closest to the real axis, coincide. At temperatures less than T_* there could also be additional dynamical temperature scales. For a local symmetry we also expect analogous phenomenology with the Goldstone mode replaced by the longitudinal mode of the massive vector. It would be interesting to compute the pole structure in other models [42], including non-conformal geometries, and to explore the ramifications in experiment. Recent experiments using cold atomic gases [4] suggest the possibility of investigating the evolution of the excitation spectrum.

[1] T. Kinoshita, T. Wenger, and D. S. Weiss, Nature **440**, 900 (2006).

[2] L. E. Sadler, J. M. Higbie, S. R. Leslie, M. Vengalattore, and D. M. Stamper-Kurn, Nature **443**, 312 (2006).

[3] R. P. Smith, S. Beattie, S. Moulder, R. L. D. Campbell, and Z. Hadzibabic, `arXiv:1112.4457`.

[4] M. Endres, T. Fukuhara, D. Pekker, M. Cheneau, P. Schauβ, C. Gross, E. Demler, S. Kuhr, and I. Bloch,

Nature (London) **487**, 454 (2012).

[5] B. Mansart, J. Lorenzana, M. Scarongella, M. Chergui, and F. Carbone, arXiv:1112.0737.

[6] P. Calabrese and J. Cardy, Phys. Rev. Lett. **96**, 136801 (2006).

[7] G. Vidal, Phys. Rev. Lett. **91**, 147902 (2003).

[8] S. R. White and A. E. Feiguin, Phys. Rev. Lett. **93**, 076401 (2004).

[9] A. J. Daley, C. Kollath, U. Schollwöck, and G. Vidal, J. Stat. Mech. , P04005 (2004).

[10] A. Polkovnikov, K. Sengupta, A. Silva, and M. Vengalattore, Rev. Mod. Phys. **83**, 863 (2011).

[11] R. A. Barankov, L. S. Levitov, and B. Z. Spivak, Phys. Rev. Lett. **93**, 160401 (2004).

[12] E. A. Yuzbashyan, O. Tsyplyatyev, and B. L. Altshuler, Phys. Rev. Lett. **96**, 097005 (2006).

[13] E. A. Yuzbashyan, B. L. Altshuler, V. B. Kuznetsov, and V. Z. Enolskii, J. Phys. A **38**, 7831 (2005).

[14] R. A. Barankov and L. S. Levitov, Phys. Rev. Lett. **93**, 130403 (2004).

[15] A. V. Andreev, V. Gurarie, and L. Radzihovsky, Phys. Rev. Lett. **93**, 130402 (2004).

[16] R. A. Barankov and L. S. Levitov, Phys. Rev. Lett. **96**, 230403 (2006).

[17] A. F. Volkov and Sh. M. Kogan, Sov. Phys. JETP **38**, 1018 (1974).

[18] V. Gurarie, Phys. Rev. Lett. **103**, 075301 (2009).

[19] J. M. Maldacena, Adv. Theor. Math. Phys. **2**, 231 (1998).

[20] S. S. Gubser, I. R. Klebanov, and A. M. Polyakov, Phys. Lett. B **428**, 105 (1998).

[21] E. Witten, Adv. Theor. Math. Phys **2**, 253 (1998).

[22] U. H. Danielsson, E. Keski-Vakkuri, and M. Kruczenski, Nucl. Phys. B **563**, 279 (1999).

[23] S. B. Giddings and S. F. Ross, Phys. Rev. D **61**, 024036 (2000).

[24] S. Bhattacharyya and S. Minwalla, JHEP **0909**, 034 (2009).

[25] S. R. Das, T. Nishioka, and T. Takayanagi, JHEP **1007**, 071 (2010).

[26] T. Albash and C. V. Johnson, New J. Phys. **13**, 045017 (2011).

[27] J. Sonner and A. G. Green, arXiv:1203.4908.

[28] P. M. Chesler and L. G. Yaffe, Phys. Rev. Lett. **102**, 211601 (2009).

[29] K. Murata, S. Kinoshita, and N. Tanahashi, JHEP **1007**, 050 (2010).

[30] P. Bizon and A. Rostworowski, Phys. Rev. Lett. **107**, 031102 (2011).

[31] D. Garfinkle and L. A. Pando Zayas, Phys. Rev. D **84**, 066006 (2011).

[32] H. Bantilan, F. Pretorius, and S. S. Gubser, Phys. Rev. D **85**, 084038 (2012).

[33] A. Buchel, L. Lehner, and R. C. Myers, arXiv:1206.6785.

[34] S. S. Gubser, Phys. Rev. D **78**, 065034 (2008).

[35] S. A. Hartnoll, C. P. Herzog, and G. T. Horowitz, Phys. Rev. Lett. **101**, 031601 (2008).

[36] S. A. Hartnoll, Class. Quant. Grav. **26**, 224002 (2009).

[37] J. McGreevy, Adv. High Energy Phys. , 723105 (2010).

[38] We can also consider the alternative quantisation with $\Delta = 1$ and we expect analogous results.

[39] S. S. Gubser, C. P. Herzog, S. S. Pufu, and T. Tesileanu, Phys.Rev.Lett. **103**, 141601 (2009).

[40] I. Amado, M. Kaminski, and K. Landsteiner, JHEP **0905**, 021 (2009).

[41] E. Berti, V. Cardoso, and A. O. Starinets, Class. Quant. Grav. **26**, 163001 (2009).

[42] See [43] for a recent calculation of the spectral properties of the O(N) model at zero temperature.

[43] D. Podolsky and S. Sachdev, arXiv:1205.2700.